



Biomimetic silica xerogel regulates indometacin release and oral bioavailability by virtue of chiral pores

Tong Lu^a, Guojie Li^b, Jing Li^{a,*}

^a School of Basic Medical Science, Shenyang Medical College, No. 146 Huang He North Street, Shenyang, Liaoning Province, China

^b College of Applied Technology, Shenyang University of Chemical Technology, No.13 Street, Tiexi Economic and Technological Development Zone, Shenyang, Liaoning Province, China

ARTICLE INFO

Keywords:

Silica xerogel
Chiral porous size distribution
Biomimetic synthesis
Delivery effect

ABSTRACT

Chiral materials exert special functions to be studied. To explore the chiral porous drug delivery effect of silica xerogel that synthesized using biomimetic method, two carriers with different chirality (BSX-CL and BSX-CD) were prepared. Morphology and porous size distribution of BSX-CL and BSX-CD were characterized. After loading indometacin into the two carriers, systemic physical state was studied using fourier transform infrared spectroscopy (FTIR) and differential scanning calorimeter (DSC) before measuring in vitro dissolution and in vivo pharmacodynamics. The results showed that BSX-CL was small sphere nanoparticles while BSX-CD turned out to be solid interlaced networks. Their distinguished morphology differences were mainly attributed to the function of small chiral molecules, resulting in the relative large mesopores of BSX-CL highly centralized within 5–10 nm, while that of BSX-CD mainly gathered within 6–13 nm. Indometacin was amorphous state in the two carriers, leading to the enhancement of in vitro drug dissolution and oral bioavailability. The relative bioavailability of indometacin loaded BSX-CL and indometacin loaded BSX-CD achieved 1.27 times and 1.87 times higher than indometacin. To summarize, BSX-CL and BSX-CD regulated indometacin release and oral bioavailability via controlling the porous size distribution.

1. Introduction

Amorphous silica has been widely applied in establishing drug delivery systems owing to its characteristics, including non-toxic, good biocompatibility and biodegradability, rigid frame, high stability, abilities of loading and delivering drugs [1–5]. Among various kinds of amorphous silica, silica xerogel has been long recognized as drug carrier according to previous reports. Silica xerogel is formed after undergoing from sol of a colloidal suspension system to gel. After gelatinization, wet gel is initially formed into a globally connected solid matrix. Xerogel is obtained after drying gel [6]. In silica sol system, many determined factors, such as pH, polarity, the involved small molecules or polymers and its volume, should be seriously considered when designing its drug loading system. The matrix of silica xerogel can be rendered as drug repository and therefore the property of matrix is a crucial influencing factor for managing drug delivery effect. Generally, drug molecules can be incorporated into silica matrix through two methods, which are in situ loading method and post adsorption method [7]. Their advantages can be described as high efficiency of drug loading and highly dispersed

drug distribution in the silica matrix, respectively. It has been reported that a large number of drugs, either water-soluble or poorly water-soluble, can be loaded into silica xerogel to perform scheduled drug delivery effect, examples were seen with nifedipine, heparin [8], propranolol hydrochloride, levofloxacin hydrochloride, metformin hydrochloride and toremifene citrate [6] as model drugs.

Instead, a variety of additives consisting of polypeptides, polysaccharides, peptides and polyamines, are able to shoulder the responsibility of forming biomimetic synthesized silica. The outstanding advantages of biomimetic synthesized silica include: (1) the whole process accomplishes at ambient working conditions, including normal temperature, normal pressure and static state without stirring, which can save much energy [9]; (2) easy and facile ways to manage the process by regulating pH, polarity, polymer concentration and other additives in the system. It has been reported that poly(ethyleneimine)s (PEIs) that belongs to polyamines can be the template for forming biomimetic synthesized silica. PEIs consist of branched PEIs and linear PEIs, which can be obtained from the ring-opening polymerization of cyclic ethyleneimine and hydrolysis of linear polyoxazoline, respectively.

* Corresponding author.

E-mail address: dddefghijklmn@163.com (J. Li).

<https://doi.org/10.1016/j.micromeso.2019.109834>

Received 5 September 2019; Received in revised form 7 October 2019; Accepted 25 October 2019

Available online 26 October 2019

1387-1811/© 2019 Elsevier Inc. All rights reserved.

Branched PEIs were normally used for preparing silica materials owing to its nontoxicity at low molecular weight (<25kD) [10,11].

As we all know, chirality is the nature property in the universe. Chiral characteristics of chiral drugs are important determinants for their bioavailability in oral drug delivery systems. For example, the bioavailability of levofolic acid is approximately 100% and that of dextrofollic acid is only 20% when orally administrating racemic folic acid. Notably, chiral materials exert special functions, typically as chiral recognition and matching ability, when being applied in biological environment [12]. It has been reported that chiral nanofibers constructed by chiral amino acids had different adhesion to cells. Therefore, it is feasible to establish chiral drug delivery systems based on chiral silica materials, which is of great research value and a new breakthrough in the materials science and drug delivery systems. For the first time, the present work synthesized a type of chiral silica materials using biomimetic method, which was biomimetic silica xerogel with chiral pores that named as BSX-C (levorotatory chiral or dextral chiral BSX-C were named as BSX-CL or BSX-CD, respectively). Branched PEIs was taken as biomimetic template and the reaction occurred at mild conditions.

To explore the chiral porous drug delivery management of BSX-C, poorly water soluble indometacin was taken as model drug. Indometacin belongs to nonsteroidal anti-inflammatory drug with poor solubility, and its applications are mainly covering acute and chronic rheumatoid arthritis, gout arthritis and cancer pain [13–16]. It can also be used for bursitis, tenosynovitis and joint bursitis. What is more, it is effective for colic caused by ureteral calculi, migraines and menstrual cramps. Indometacin was loaded into BSX-CL or BSX-CD through in situ loading method. Indometacin, BSX-CL, BSX-CD, Indometacin loaded BSX-CL and indometacin loaded BSX-CD were characterized using fourier transform infrared spectroscopy (FTIR), scanning electron microscopy (SEM), nitrogen adsorption/desorption and differential scanning calorimeter (DSC). In the end, in vitro release behavior and in vivo pharmacokinetic studies were carried out to reveal how BSX-CL and BSX-CD regulate drug release with chiral porous control manner.

2. Materials and methods

2.1. Materials

Tetramethoxysilane (TMOS) was purchased from Aladdin (Shanghai, China), branched poly(ethyleneimine)s (PEIs) with weight-average molecular weight of 20000 was kindly donated by Qianglong new chemical materials (Wuhan, China). All other chemical were of reagent grade and deionized water was prepared by ion exchange.

The laboratory animal experiment was conducted according to the ethical guidelines that approved by the Ethics Review Committee for Animal Experimentation of Shenyang Medical College (Shenyang, China).

2.2. Preparation of BSX-CL and BSX-CD

BSX-CL and BSX-CD were synthesized using the similar working conditions. The brief preparation process of BSX-CL was described as follows. Initially, small chiral molecular solution with concentration of 50 g/L was prepared by dissolving L-tartaric acid in deionized water. PEIs aggregate solution was prepared by mixing PEIs with deionized water to get the final PEIs concentration of 1.0 wt%. Afterwards, 0.5 mL TMOS was mixed with 0.4 mL absolute ethyl alcohol, followed by adding small chiral molecular solution, APTES and PEIs aggregate solution with volume ratio of 0.5:0.5:0.2. The system was left at ambient condition statically until the formation of wet gel. Finally, organic solvent inside the system was evaporated at room temperature until xerogel state. BSX-CD was obtained using the same preparation process except that D-tartaric acid was applied as small chiral molecular agent.

2.3. Loading indometacin into BSX-C

There are two methods normally applied to load drug molecules into silica carriers, which are in situ loading method (one-pot drug inclusion method) and post drug adsorption method [7]. By adopting in situ loading method, desired amount of drug was impregnated into silica carriers, which was easy and efficient with no need to calculate drug loading amount as well as drug loading efficiency. Herein, a certain amount of indometacin was dissolved in absolute ethyl alcohol. 0.5 mL TMOS was mixed with 0.2 mL absolute ethyl alcohol, followed by adding indometacin anhydrous ethanol solution, small chiral molecular solution, APTES and PEIs aggregate solution with volume ratio of 0.2:0.5:0.5:0.2. The system was left at ambient condition statically until the formation of wet gel. Finally, organic solvent inside the system was evaporated at room temperature until xerogel state.

2.4. Morphology and porous structure of carriers

2.4.1. SEM

SEM was obtained with SURA 35 field emission scanning electron microscope (ZEISS, Germany) to analyze surface morphology of BSX-CL and BSX-CD. Samples were mounted onto metal stubs using double-sided adhesive tape and sputtered with a thin layer of gold under vacuum.

2.4.2. Porous distribution analysis

According to a large number of literatures that studied silica materials as drug carrier, the porous size was the main determination for managing drug release manner. Therefore, the porous size distribution, specific surface area and pore volume of BSX-CL and BSX-CD were studied by nitrogen adsorption and desorption measurement using V-Sorb 2800P (app-one, China). All samples were degassed at 50 °C vacuum drying for sufficient time prior to analysis to remove adsorbed water.

2.5. Verification physical state of indometacin inside carriers

2.5.1. FTIR

Fourier transform infrared spectroscopy (FT-IR, Spectrum 1000, PerkinElmer, USA) spectra of samples were obtained over the spectral region 400 to 4000 cm^{-1} . Samples were prepared by gently and respectively grounding with KBr.

2.5.2. DSC

Thermal analysis was conducted by utilizing differential scanning calorimeter (DSC, Q1000, TA Instrument, USA). Samples were placed in pierced aluminum pans and heated from 30 to 300 °C at a scanning rate of 10 °C/min under nitrogen protection.

2.6. Wetting property and drug release

2.6.1. Contact angle measurement

The contact angle was conducted using JCY series (Shanghai, China). Automatic contact angle meter model was applied for measurement. 200 mg powder was weighed and compressed using a circular stainless steel punch and die in a infrared tablet press for 10 s at high pressure. A drop of dissolution medium contacted compressed plate and the initial contact angle was measured [17].

2.6.2. In vitro dissolution

Drug release experiment was carried out using small paddle method (100 rpm, 37 °C, and 250 ml dissolution medium) with a ZRD6-B dissolution tester (Shanghai Huanghai Medicament Test Instrument Factory, China). Indometacin, indometacin loaded BSX-CL and indometacin loaded BSX-CD were exposed to enzyme-free simulated intestinal fluid (pH 6.8). At predetermined time intervals, 5 ml samples were

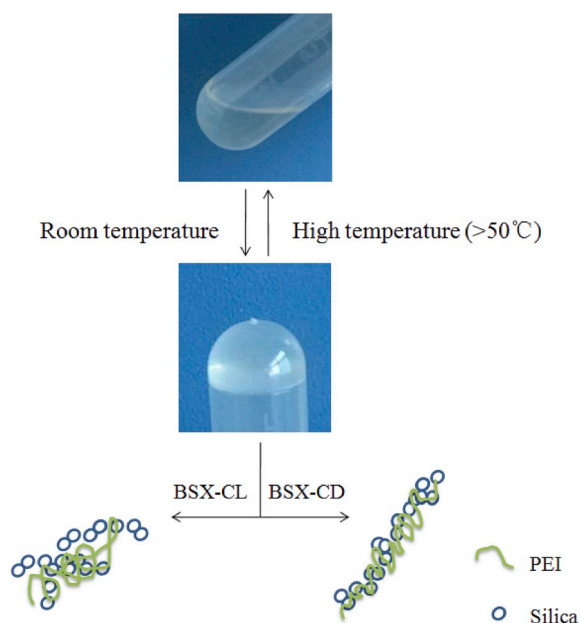


Fig. 1. Photo of BSX-C during sol to gel process and schematic illustration of different systemic inside state of BSX-CL and BSX-CD.

withdrawn from the release medium and then an equivalent amount of fresh medium was added to maintain a constant dissolution volume. Samples administered through $0.45\ \mu\text{m}$ microporous membrane were analyzed using UV-1750 (Shimadzu, Japan) at the wavelength of 320 nm.

2.7. In vivo pharmacokinetics

Male Wistar rats weighing $200 \pm 20\ \text{g}$ were randomly divided into three groups (A group, indometacin; B group, indometacin loaded BSX-CL; C group, indometacin loaded BSX-CD) with three animals in each group. All the rats were fasted for 12 h but allowed to get water before experiment. Sample solutions with dose of 8 mg/body weight were orally administered to corresponding groups of rats. Blood of each animal was collected via the suborbital vein at different time intervals and then immediately centrifuged at 5000 rpm to collect plasma. 200 μL plasma was mixed with 10 μL internal standard 0.3 mg/mL naproxen solution, 90 μL 10% K_2HPO_4 (pH 3.0) and 1 mL dichloromethane. The mixture was vortexed for 3 min and centrifuged at 10000 rpm for 4 min. The above aqueous phase was removed and the organic phase was dried under nitrogen protection. 100 μL mobile phase was added to redissolve samples and the supernatant of each sample was subjected to HPLC analysis.

3. Results and discussions

3.1. Preparation process and mechanism

The formation mechanism of BSX-CL and BSX-CD can be concluded as the aggregation of PEI, polycondensation of silica source to form silica frame, transformation from silica sol to silica gel and finally silica xerogel. During the formation process of silica sol to silica gel, the systemic viscosity gradually increased. The turning point ascribed to the establishment of silica network structure with sufficient strength. Gel state failed to be obtained if the gel strength was not strong enough to remain the solvent within silica frame. The special discovery for the synthesis of BSX-CL and BSX-CD was that the sol to gel process belonged to reversible reaction (see Fig. 1), which meant the transformation of sol

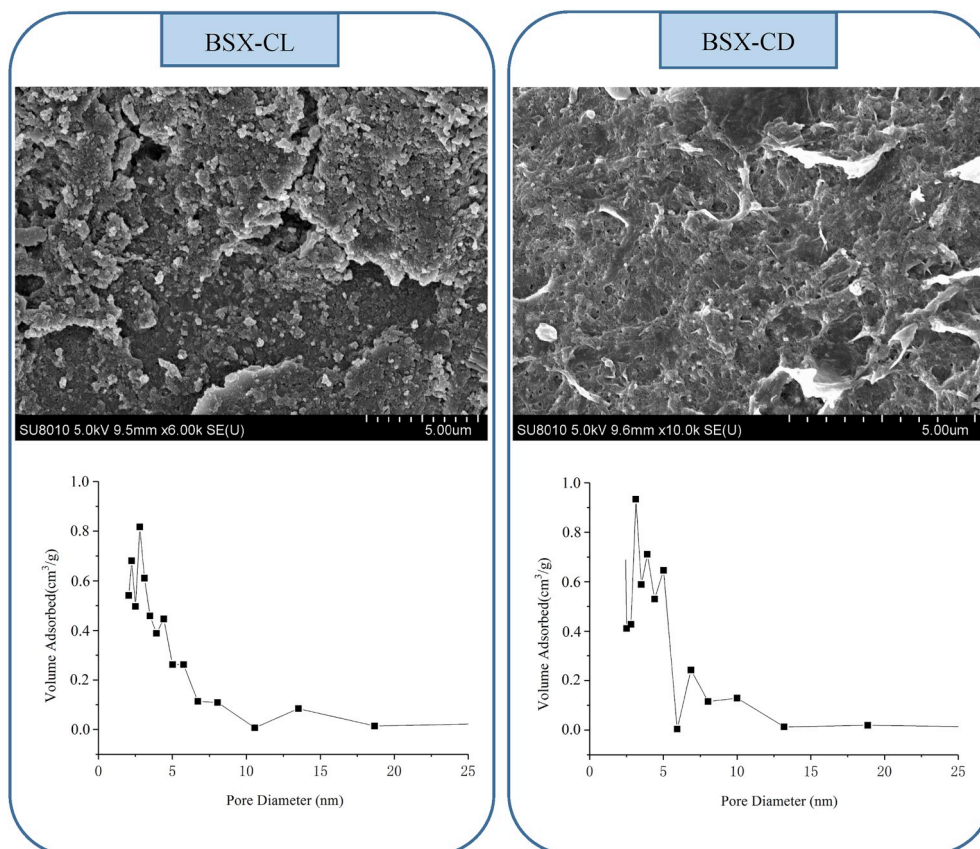


Fig. 2. SEM images and porous size distribution curves of BSX-CL and BSX-CD.

to gel accomplished at room temperature while gel state can be turned to sol phase at high temperature (above 50 °C). This phenomenon reflected the thermosensitivity of BSX-CL and BSX-CD owing to the approximate half volume ratio of aqueous solution and the thorough dispersion of PEI in the system. Therefore, high temperature (above 50 °C) should not be used during the formation of silica gel. However, after silica xerogel was obtained, high temperature condition was proper to be used to evaporate residual organic solvent. Notably, both PEI and APTES exerted catalysis functionalities owing to their amino groups. After forming silica xerogel, a large number of silanol groups together with amino groups originating from PEI and APTES contributed to be active sites for interacting with newcomers for loading drug or realizing surface modification [18]. In the two synthesized systems, small chiral molecules endowed porous channels with chiral property because these small chiral molecules interacted with the amino groups of APTES to control silica condensation and therefore affected the formation of silica frame and porous structure. Different from other surface modified silica materials, BSX-CL and BSX-CD were surface modified with carboxyl and amino groups and also chirally modified.

3.2. SEM

SEM images of BSX-CL and BSX-CD were shown in Fig. 2. It was obvious that BSX-CL presented small sphere nanoparticles while BSX-CD turned out to be solid interlaced networks. Their distinguished morphology differences were mainly attributed to the function of small chiral molecules in regulating the aggregation state of PEI in the system. Dextral small molecules were capable of strengthening the extended state of PEI owing to the interface forces between carboxyl groups with amino groups and most of natural substance was clockwise formed, further leading to the silica condensation with sufficient time to form interlaced networks. On the contrary, levorotatory small molecules did not form strong interaction with PEI and therefore PEI failed to spread with high extensibility, resulting in silica condensation with sphere particle structure. It was interesting that small chiral molecules can obviously affect materials morphology, which turned out to be an important discovery in the study of chiral silica materials, confirming that this parameter was crucial in silica formation process. Since BSX-CL and BSX-CD displayed distinguished differences in morphology, whether their porous size distributions were different or not remained to be seen.

3.3. Nitrogen adsorption/desorption measurement

For a large number of silica materials as drug carriers, porous size was the determined factor for controlling drug delivery behavior [19–21]. Normally, fast drug release rate and high cumulative drug release amount can be obtained from silica carriers with large porous size since the large pores provided wide space for drug molecules to escape from the carrier restraint. Herein, the porous size distributions of BSX-CL and BSX-CD were measured, which can be seen in Fig. 2. Generally, their porous size distribution profiles presented two-stage of distribution within mesoporous size (<50 nm), which can be divided into one stage of relative small mesopores (<5 nm) and the other stage of relative large mesopores (>5 nm). The two-stage porous size distributions of BSX-CL and BSX-CD showed different curve patterns. The most important point can be concluded as that BSX-CL displayed smaller porous size of relative large mesopores compared with BSX-CD, reflecting their different distribution ratios of relative large mesopores and relative small mesopores. To be specific, the relative large mesopores of BSX-CL highly centralized in the range of 5–10 nm, while the relative large mesopores of BSX-CD mainly gathered within 6–13 nm. The different distributions of relative large mesopores were closely related with their formation mechanism. Due to small chiral molecules was the main different factor during the formation of these two carriers, their porous size distributions were ascribed to the functions of small

Table 1

In vivo pharmacokinetic parameters of indometacin, indometacin loaded BSX-CL and indometacin loaded BSX-CD.

| Parameters | Indometacin | Indometacin loaded BSX-CL | Indometacin loaded BSX-CD |
|---|------------------|---------------------------|---------------------------|
| AUC _(0-t) (μg/mL ² h) | 458.654 ± 26.375 | 582.671 ± 64.365 | 857.638 ± 73.368 |
| MRT _(0-t) (h) | 9.414 ± 0.503 | 9.332 ± 0.115 | 8.911 ± 0.953 |
| t _{1/2z} (h) | 6.673 ± 1.836 | 17.011 ± 2.137 | 19.792 ± 18.444 |
| T _{max} (h) | 6.000 ± 0.000 | 6.000 ± 0.000 | 6.000 ± 0.000 |
| C _{max} (μg/mL) | 35.144 ± 2.321 | 66.201 ± 10.386 | 86.959 ± 4.095 |

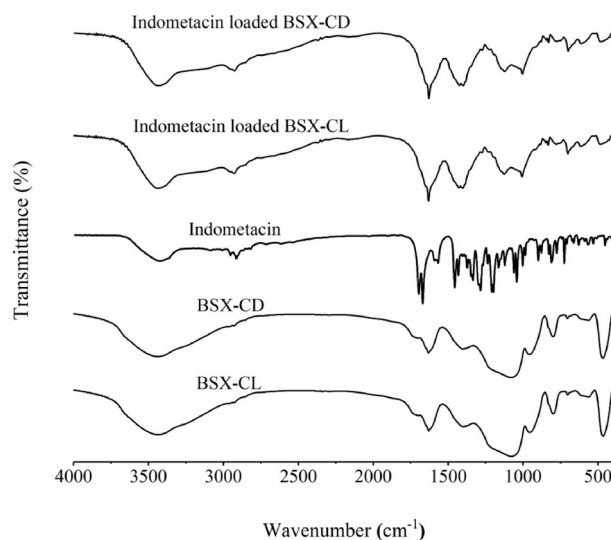


Fig. 3. IR spectra of BSX-CL, BSX-CD, indometacin, indometacin loaded BSX-CL and indometacin loaded BSX-CD.

chiral molecules. As stated previously, dextral small molecules were capable of strengthening the extended state of PEI and further leading to the silica condensation with sufficient time to form interlaced networks, while levorotatory small molecules failed to facilitate the spread of PEI with high extensibility and resulted in silica condensation with sphere particle structure. Therefore, BSX-CD with higher level of interlaced networks comprised of relative large mesopores that mainly gathered in larger porous range, while the relative large mesopores of BSX-CL centralized in relative lower porous range (see illustration graph in Fig. 2). The clear elucidation of formation mechanism, morphology and porous size distribution of BSX-CL and BSX-CD solidified the comprehension of biomimetic silica xerogel with chiral property. In addition, specific surface area and pore volume of BSX-CL and BSX-CD were provided in Supporting information Table 1 and their nitrogen adsorption/desorption isotherms were shown in Supporting information Fig. 1. It demonstrated that the specific surface area and pore volume of BSX-CD were a little larger than BSX-CL, while the difference was not significant, which further confirmed the crucial role of porous size distribution for the two carriers.

3.4. FTIR

As shown in Fig. 3, infrared spectra of BSX-CL and BSX-CD presented characteristic peaks belonging to silica xerogel, including Si–O–Si bending vibration at 465.1 cm⁻¹ and 465.6 cm⁻¹, Si–O–Si symmetric stretching vibration at 798.4 cm⁻¹ and 798.7 cm⁻¹, Si–O–Si antisymmetric stretching vibration at 1079.6 cm⁻¹ and 1079.9 cm⁻¹ [22], -COO- stretching vibration at 1400.9 cm⁻¹ and 1401.1 cm⁻¹, N–H deformation vibration at 1630.2 cm⁻¹ and 1630.5 cm⁻¹, OH of Si–OH antisymmetric stretching vibration at 3439.7 cm⁻¹ and 3439.5 cm⁻¹.

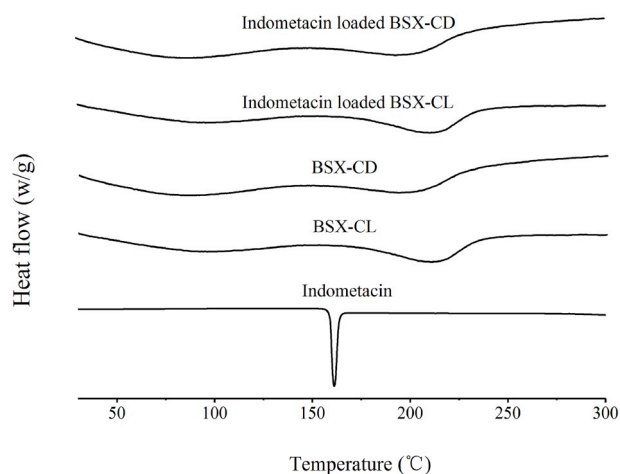
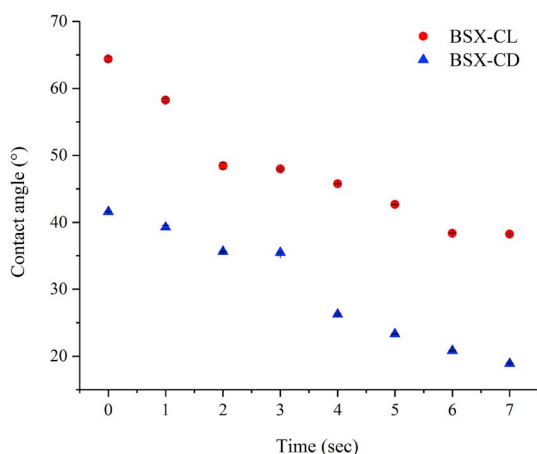
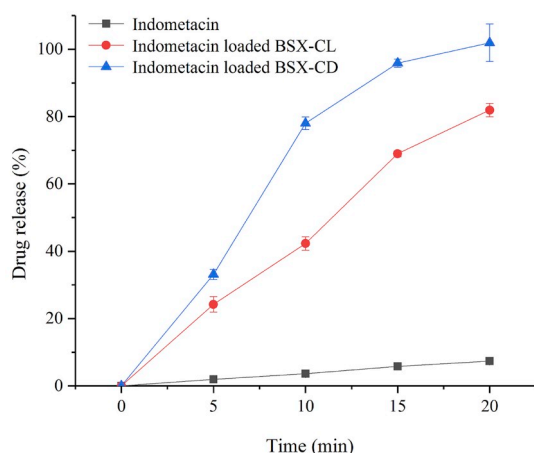


Fig. 4. DSC curves of indometacin, BSX-CL, BSX-CD, indometacin loaded BSX-CL and indometacin loaded BSX-CD.



A



B

Fig. 5. A, Contact angle of BSX-CL and BSX-CD; B, In vitro dissolution of indometacin, indometacin loaded BSX-CL and indometacin loaded BSX-CD.

Infrared spectroscopy of Indometacin showed its classical characteristic peaks at 1717.3 and 1691.0 cm^{-1} that assigned to the carbonyl groups of the acid and amide, peak at 1308.0 cm^{-1} belonging to aromatic C–N

stretching vibration, and peak at 1140.7 cm^{-1} of C–O–C stretching vibration. After loading indometacin into BSX-CL and BSX-CD, classical drug peaks of carbonyl groups and aromatic C–N stretching vibration had been covered, demonstrating that BSX-CL and BSX-CD were effective in encapsulating small drug molecules. In addition, the displayed peaks of N–H deformation vibration, –COO– stretching vibration and Si–O–Si antisymmetric stretching vibration that belonged to the two carriers had been blue shifted, while the drug classical peak of C–O–C stretching vibration showed red shifted, confirming that hydrogen bonds were formed between drug with the two carriers. The formed hydrogen bonds turned out to be the favourable factor for establishing drug loaded carrier systems and influencing the crystalline state of loaded drug.

3.5. DSC

Drug crystalline state can be also demonstrated by conducting DSC experiment [23,24]. DSC thermograms of BSX-CL and BSX-CD showed endothermic phenomena but not obvious endothermic peaks (Fig. 4), indicating that branched PEIs known as amorphous polyamine, was adsorbed onto amorphous silica. It is known to all that crystalline silica can cause a rapid influx of inflammatory cells, increase collagen deposition in lungs, and change histological state of pulmonary lymph nodes [25], therefore BSX-CL and BSX-CD were safe to be drug carriers due to amorphous state of silica [10]. As shown in Fig. 4, the DSC curve of indometacin exhibited a single endothermic peak at 160.54 $^{\circ}\text{C}$, which corresponded to its intrinsic melting points. However, no melting peak of indometacin was identified in the DSC curves obtained from indometacin loaded BSX-CL or indometacin loaded BSX-CD. The absence of phase transitions owing to indometacin in the DSC analysis was evidence that indometacin was in amorphous state [26–28]. The amorphous phase of indometacin was favourable for improving drug dissolution since the loaded amorphous drug had higher energy compared with crystalline drug to release into the medium.

3.6. Wetting property of carriers and drug release

For most of solid formulations, wetting property with ability to reflect the water penetration level of excipient is an important point should be considered. As shown in Fig. 5A, the overall contact angle of BSX-CD was significantly lower than BSX-CL, which illustrated that the larger porous range of relative large mesopores from BSX-CD contributed to its enhanced water penetration level than BSX-CL. Furthermore, the contact angle spots of BSX-CL and BSX-CD displayed two stages (the first stage of BSX-CL was in the range of 0–2 s and the second stage was within 2–7 s, while the first stage of BSX-CD was in the range of 0–3 s and the second stage was within 3–7 s), possibly can be ascribed to the two-stage distributions of mesopores in the two carriers.

It has been well acknowledged that the release mechanism of silica xerogel can be concluded as diffusion and erosion [6]. As can be seen in Fig. 5B, drug dissolution of both indometacin loaded BSX-CL and indometacin loaded BSX-CD had been significantly improved evidenced by their obvious higher drug release profiles than indometacin. The enhancement of drug dissolution was attributed to the amorphous phase of indometacin in the carrier matrix that proved by DSC measurement since its high energy facilitated drug release. What is more, the cumulative drug release of indometacin loaded BSX-CL and indometacin loaded BSX-CD at 20 min reached almost 80% and 100% respectively, demonstrating that BSX-CD with superior wetting property based on its larger porous range of relative large mesopores than BSX-CL was beneficial for releasing drug molecules, which was in agreement with the widely accepted principle that fast drug release can be achieved by applying silica with large mesopores [27]. The enhancement of drug dissolution was crucial for indometacin because poorly water-solubility was the main limiting factor of drug release.

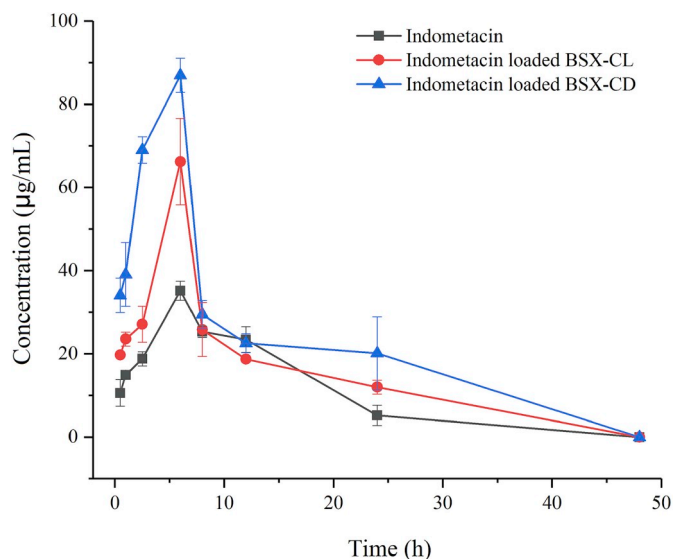


Fig. 6. In vivo pharmacokinetic profiles of indometacin, indometacin loaded BSX-CL and indometacin loaded BSX-CD.

3.7. In vivo pharmacokinetic studies

In vivo pharmacokinetic profiles and parameters were shown in Fig. 6 and Table 1. It was obvious that BSX-CL and BSX-CD had advantages in improving indometacin bioavailability evidenced by their enhanced C_{max} and AUC. The C_{max} of indometacin, indometacin loaded BSX-CL and indometacin loaded BSX-CD turned out to be 35.144 µg/mL, 66.201 µg/mL and 86.959 µg/mL, respectively. The mean AUC values of indometacin loaded BSX-CL and indometacin loaded BSX-CD reached to 582.671 µg/mL and 857.638 µg/mL, which were 1.27 times and 1.87 times higher than mean AUC value of indometacin. The oral bioavailability enhancement was obtained because amorphous phase of indometacin in carriers had higher dissolution than crystalline indometacin [29–32]. Furthermore, the oral bioavailability of indometacin loaded BSX-CD was better than indometacin loaded BSX-CL, which was in agreement with in vitro drug release result, demonstrating that the large porous range of relative large mesopores was superior in improving dissolution of poorly water-soluble drug and further enhancing oral bioavailability.

4. Conclusions

BSX-CL and BSX-CD that surface modified with carboxyl groups and amino groups had been successfully synthesized using biomimetic synthesis method and possessed chirality. According to the results of a series of measurement, BSX-CL presented small sphere nanoparticles while BSX-CD turned out to be solid interlaced networks. Their distinguished morphology differences were mainly attributed to the function of small chiral molecules in regulating the aggregation state of PEI in the system, further leading to the relative large mesopores of BSX-CL highly centralized in the range of 5–10 nm, while the relative large mesopores of BSX-CD mainly gathered within 6–13 nm. BSX-CL and BSX-CD were effective in encapsulating small drug molecules and hydrogen bonds were formed between indometacin with the two carriers. DSC curves obtained from indometacin loaded BSX-CL or indometacin loaded BSX-CD showed no drug melting peak, confirming that indometacin was in amorphous state. The conversion of drug crystalline state contributed to the enhancement of in vitro drug dissolution, and BSX-CD with superior wetting property based on its larger porous range of relative large mesopores than BSX-CL was beneficial for releasing drug molecules. In vivo, the relative bioavailability of indometacin loaded BSX-CL and indometacin loaded BSX-CD achieved 1.27 times and 1.87 times higher

than indometacin. To summarize, BSX-CL and BSX-CD regulated indometacin release and oral bioavailability via controlling the porous size distribution. BSX-CD with large porous range of relative large mesopores was superior in improving dissolution of poorly water-soluble drug and further enhancing oral bioavailability.

Declaration of competing interest

The authors declare that they have no known competing financial interests or personal relationships that could have appeared to influence the work reported in this paper.

Appendix A. Supplementary data

Supplementary data to this article can be found online at <https://doi.org/10.1016/j.micromeso.2019.109834>.

References

- [1] F. L. Xinxin Zhang, Shiyun Guo, Xi Chen, Xiaoli Wang, Juan Li, Yong Gan, Biofunctionalized polymer-lipid supported mesoporous silica nanoparticles for release of chemotherapeutics in multidrug resistant cancer cells, *Biomaterials* 35 (2014) 3650–3665.
- [2] N. Song, Y.W. Yang, Molecular and supramolecular switches on mesoporous silica nanoparticles, *Chem. Soc. Rev.* 44 (2015) 3474–3504.
- [3] Q.L. Li, S.H. Xu, H. Zhou, X. Wang, B. Dong, H. Gao, J. Tang, Y.W. Yang, pH and glutathione dual-responsive dynamic cross-linked supramolecular network on mesoporous silica nanoparticles for controlled anticancer drug release, *ACS Appl. Mater. Interfaces* 7 (2015) 28656–28664.
- [4] J.Y. Choi, T. Ramasamy, S.Y. Kim, J. Kim, S.K. Ku, Y.S. Youn, J.R. Kim, J.H. Jeong, H.G. Choi, C.S. Yong, J.O. Kim, PEGylated lipid bilayer-supported mesoporous silica nanoparticle composite for synergistic co-delivery of axitinib and celestrol in multi-targeted cancer therapy, *Acta Biomater.* 39 (2016) 94–105.
- [5] Q. Y. Yu Zhang, Moustafa M. Zagho, Jiajie Zhang, Ahmed A. Elzatahry, a.Y. D, Yongjian Jiang, Core-shell magnetic mesoporous silica microspheres with large mesopores for enzyme immobilization in biocatalysis, *ACS Appl. Mater. Interfaces* 11 (2019) 10356–10363.
- [6] M. Ahola, P. Korteso, I. Kangasniemi, J. Kiesvaara, A. Yli-Urpo, Silica xerogel carrier material for controlled release of toremifene citrate, *Int. J. Pharm.* 195 (2000) 219–227.
- [7] J. Li, L. Xu, H. Liu, Y. Wang, Q. Wang, H. Chen, W. Pan, S. Li, Biomimetic synthesized nanoporous silica@poly(ethyleneimine)s xerogel as drug carrier: characteristics and controlled release effect, *Int. J. Pharm.* 467 (2014) 9–18.
- [8] M.S. Ahola, E.S. Säilynoja, M.H. Raitavu, M.M. Vaahtio, J.I. Salonen, A.U. Yli-Urpo, In vitro release of heparin from silica xerogels, *Biomaterials* 22 (2001) 2163–2170.
- [9] S.V. Patwardhan, Biomimetic and bioinspired silica: recent developments and applications, *Chem. Commun* 47 (2011) 7567–7582.
- [10] T. Xia, M. Kovochich, M. Liong, H. Meng, S. Kabehie, S. George, J.I. Zink, A.E. Nel, Polyethyleneimine coating enhances the cellular uptake of mesoporous silica nanoparticles and allows safe delivery of siRNA and DNA constructs, *ACS Nano* 3 (2009) 3273–3286.
- [11] H.W. Jing Li, Heran Li, Lu Xu, Yingyu Guo, Fangzheng Lu, Weisan Pan, S. Li, Mutual interaction between guest drug molecules and host nanoporous silica xerogel studied using central composite design, *Int. J. Pharm.* 498 (2016) 32–39.
- [12] F.Z. Jiahua Zhou, Jing Li*, Yongjun Wang, Concealed body mesoporous silica nanoparticles for orally delivering indometacin with chiral recognition function, *Mater. Sci. Eng. C* 90 (2018) 314–324.
- [13] J. Li, L. Xu, H. Wang, B. Yang, H. Liu, W. Pan, S. Li, Comparison of bare and amino modified mesoporous silica@poly(ethyleneimine)s xerogel as indometacin carrier: superiority of amino modification, *Mater. Sci. Eng. C* 59 (2016) 710–716.
- [14] T.V. Duong, J. Van Humbeeck, G. Van den Mooter, Crystallization kinetics of indometacin/polyethylene glycol dispersions containing high drug loadings, *Mol. Pharm.* 12 (2015) 2493–2504.
- [15] J. Li, L. Xu, B. Yang, Z. Bao, W. Pan, S. Li, Biomimetic synthesized chiral nanoporous silica: structures and controlled release functions as drug carrier, *Mater. Sci. Eng. C* 55 (2015) 367–372.
- [16] J. Li, L. Xu, B. Yang, H. Wang, Z. Bao, W. Pan, S. Li, Facile synthesis of functionalized ionic surfactant templated mesoporous silica for incorporation of poorly water-soluble drug, *Int. J. Pharm.* 492 (2015) 191–198.
- [17] J. Li, Y. Guo, Basic evaluation of typical nanoporous silica nanoparticles in being drug carrier: structure, wettability and hemolysis, *Mater. Sci. Eng. C* 73 (2017) 670–673.
- [18] C. Barbe, J. Bartlett, L. Kong, K. Finnie, H.Q. Lin, M. Larkin, S. Calleja, A. Bush, G. Calleja, Silica particles: a novel drug-delivery system, *Adv. Mater.* 16 (2004) 1959–1966.
- [19] Y. Wang, Q. Zhao, N. Han, L. Bai, J. Li, J. Liu, E. Che, L. Hu, Q. Zhang, T. Jiang, S. Wang, Mesoporous silica nanoparticles in drug delivery and biomedical applications, *Nanomed. Nanotechnol. Biol. Med.* 11 (2015) 313–327.

- [20] Xin Wang, Li Chang, Na Fan, Li Jing, Zhonggui He, S. Jin, Multimodal nanoporous silica nanoparticles functionalized with aminopropyl groups for improving loading and controlled release of doxorubicin hydrochloride, *Mater. Sci. Eng. C* 78 (2017) 370–375.
- [21] C.A. McCarthy, R.J. Ahern, R. Dontireddy, K.B. Ryan, A.M. Crean, Mesoporous silica formulation strategies for drug dissolution enhancement: a review, *Expert Opin. Drug Deliv.* 13 (2016) 93–108.
- [22] J. Li, Y. Guo, H. Li, L. Shang, S. Li, Superiority of amino-modified chiral mesoporous silica nanoparticles in delivering indometacin, *Artificial Cells, Nanomedicine, and Biotechnology* (2017) 1–10.
- [23] L. Yu, Amorphous pharmaceutical solids: preparation, characterization and stabilization, *Adv. Drug Deliv. Rev.* 48 (2001) 27–42.
- [24] S.A. Raina, D.E. Alonzo, G.G. Zhang, Y. Gao, L.S. Taylor, Impact of polymers on the crystallization and phase transition kinetics of amorphous nifedipine during dissolution in aqueous media, *Mol. Pharm.* 11 (2014) 3565–3576.
- [25] P. Korteso, M. Ahola, S. Karlsson, I. Kangasniemi, A. Yli-Urpo, J. Kiesvaara, Silica xerogel as an implantable carrier for controlled drug delivery—evaluation of drug distribution and tissue effects after implantation, *Biomaterials* 21 (2000) 193–198.
- [26] F. Uejo, W. Limwikrant, K. Moribe, K. Yamamoto, Dissolution improvement of fenofibrate by melting inclusion in mesoporous silica, *Asian J. Pharm. Sci.* 8 (2013) 329–335.
- [27] Y. Hu, Z. Zhi, T. Wang, T. Jiang, S. Wang, Incorporation of indomethacin nanoparticles into 3-D ordered macroporous silica for enhanced dissolution and reduced gastric irritancy, *Eur. J. Pharm. Biopharm.* 79 (2011) 544–551.
- [28] B. Tzankov, K. Yoncheva, M. Popova, A. Szegedi, G. Momekov, J. Mihály, N. Lambov, Indometacin loading and in vitro release properties from novel carbopol coated spherical mesoporous silica nanoparticles, *Microporous Mesoporous Mater.* 171 (2013) 131–138.
- [29] Y. Huang, W.-G. Dai, Fundamental aspects of solid dispersion technology for poorly soluble drugs, *Acta Pharm. Sin. B* 4 (2014) 18–25.
- [30] C. Leuner, J. Dressman, Improving drug solubility for oral delivery using solid dispersions, *Eur. J. Pharm. Biopharm.* 50 (2000) 47–60.
- [31] C.L.-N. Vo, C. Park, B.-J. Lee, Current trends and future perspectives of solid dispersions containing poorly water-soluble drugs, *Eur. J. Pharm. Biopharm.* 85 (2013) 799–813.
- [32] T. Xie, L.S. Taylor, Improved release of celecoxib from high drug loading amorphous solid dispersions formulated with polyacrylic acid and cellulose derivatives, *Mol. Pharm.* 13 (2016) 873–884.